

AperTO - Archivio Istituzionale Open Access dell'Università di Torino

**On How Differently the Quasi-harmonic Approximation Works for Two Isostructural Crystals:
Thermal Properties of MgO and CaO.**

This is the author's manuscript

Original Citation:

Availability:

This version is available <http://hdl.handle.net/2318/157348> since 2016-08-04T15:18:17Z

Published version:

DOI:10.1063/1.4906422

Terms of use:

Open Access

Anyone can freely access the full text of works made available as "Open Access". Works made available under a Creative Commons license can be used according to the terms and conditions of said license. Use of all other works requires consent of the right holder (author or publisher) if not exempted from copyright protection by the applicable law.

(Article begins on next page)



UNIVERSITÀ DEGLI STUDI DI TORINO

This is an author version of the contribution published on:

A. Erba, M. Shahrokhi, R. Moradian, R. Dovesi
On How Differently the Quasi-harmonic Approximation Works for Two
Isostructural Crystals: Thermal Properties of MgO and CaO.
THE JOURNAL OF CHEMICAL PHYSICS (2015) 142

On How Differently the Quasi-harmonic Approximation Works for Two Isostructural Crystals: Thermal Properties of Periclase and Lime.

A. Erba,^{1, a)} M. Shahrokhi,^{1, 2} R. Moradian,² and R. Dovesi¹

¹⁾*Dipartimento di Chimica, Università di Torino and NIS, Nanostructured Interfaces and Surfaces, Centre of Excellence, Via Giuria 5, 10125 Torino, Italy*

²⁾*Physics Department, Faculty of Science, Razi University, Kermanshah, Iran*

(Dated: 4 January 2015)

Harmonic and quasi-harmonic thermal properties of two isostructural simple oxides (periclase, MgO, and lime, CaO) are computed with *ab initio* periodic simulations based on the density-functional-theory (DFT). The more polarizable character of calcium with respect to magnesium cations is found to dramatically affect the validity domain of the quasi-harmonic approximation that, for thermal structural properties (such as temperature dependence of volume, $V(T)$, bulk modulus, $K(T)$ and thermal expansion coefficient, $\alpha(T)$), reduces from [0 K - 1000 K] for MgO to just [0 K - 100 K] for CaO. On the contrary, Thermodynamic properties (such as entropy, $S(T)$, and constant-volume specific heat, $C_V(T)$) are described reliably at least up to 2000 K and quasi-harmonic constant-pressure specific heat, $C_P(T)$ up to about 1000 K in both cases. The effect of the adopted approximation to the exchange-correlation functional of the DFT is here explicitly investigated by considering five different expressions of three different classes (local-density approximation, generalized-gradient approximation and hybrids). Computed harmonic thermodynamic properties are found to be almost independent of the adopted functional, whereas quasi-harmonic structural properties are largely affected by the choice of the functional, with differences that increase as the system becomes softer.

Keywords: thermal properties, thermal expansion, quasi-harmonic approximation, thermodynamic properties

I. INTRODUCTION

A wealth of information about the temperature and pressure dependence of thermodynamic properties of solids can be extracted from the knowledge of the evolution of lattice dynamics on expansion and compression. Theoretical *ab initio* simulations, based on the widely used density functional theory (DFT), do represent a powerful tool for this kind of investigations, allowing for the simultaneous description of high temperatures and pressures.¹⁻⁷

Some thermodynamic properties (such as the temperature dependence of entropy, $S(T)$, constant-volume specific heat, $C_V(T)$ and Helmholtz's free energy, $F(T)$) can be effectively computed within a harmonic description of the lattice potential. Others (such as the thermal expansion, $\alpha(T)$, the constant-pressure specific heat, $C_P(T)$, the temperature dependence of the bulk modulus, $K(T)$, the simultaneous dependence on temperature and pressure of entropy, $S(P, T)$ and Helmholtz's free energy, $F(P, T)$, etc.) require to go somehow beyond the harmonic approximation (HA).^{8,9} In this respect, the quasi-harmonic approximation (QHA) provides the simplest formal frame allowing for their calculation by introducing an explicit dependence on volume of phonon frequencies and retaining the harmonic expression for the Helmholtz free energy.^{10,11} The validity domain of the QHA (*i.e.* the temperature range where it could give a reliable description of such thermodynamic properties) can hardly

be expressed as a general function of the Debye temperature, θ_D , and melting temperature, T_M , of a material; it rather appears to be related to the chemical nature of the bond framework of the structure: in general, one might just expect that the weaker the interatomic interactions, the softer the phonon modes, the larger the intrinsic anharmonic effects and the smaller the validity domain.¹²

A major practical drawback of DFT is obviously its non-uniqueness: a huge variety of exchange-correlation functionals have been proposed, on which most computed properties dramatically depend. Different classes of functionals are commonly sorted in terms of increasing accuracy, for practical purposes, according to John Perdew's "Jacob's ladder" proposal. Local density approximation (LDA), generalized-gradient approximation (GGA), meta-GGA, hybrid and double-hybrid approaches constitute the main rungs of such a ladder. In this respect, the large majority of the quasi-harmonic calculations of solids reported so far has been performed at the LDA level.¹²⁻¹⁸ A few of them reported GGA results.^{19,20} Only very recently higher order approximations have been used in a couple of studies on diamond.^{2,21} As a consequence, the effect on computed quasi-harmonic properties of the adopted DFT approximation still has to be critically addressed, in particular for ionic materials where it is expected to be larger than for covalent ones.

A fully automated algorithm, implemented in the CRYSTAL program, has recently been presented for the *ab initio* evaluation of quasi-harmonic properties of crystals,² which is here revised and made more stable and generally applicable. The main element of novelty, in this respect, is represented by the fitting of individual phonon frequencies as a function of volume (after having estab-

^{a)}Electronic mail: alessandro.erba@unito.it

lished their continuity on volume by computing scalar products of the corresponding normal coordinates), from which all thermodynamic properties can then be easily derived. Such revised algorithm is applied to the study of the temperature dependence of a large variety of structural and thermodynamic properties (entropy, constant-volume and constant-pressure specific heat, thermal expansion, bulk modulus, etc.) of two prototypical ionic crystals such as periclase, MgO, and lime, CaO. Despite they exhibit the same structure and a similar degree of ionicity, these two crystals are found to behave quite differently as regards the effectiveness of the QHA, due to the more polarizable character of calcium cations with respect to magnesium ones.

Consolidated experimental data are available for the thermodynamic properties of MgO to compare with.²²⁻²⁴ Many experimental studies have been reported about its thermal expansion, as well,²²⁻³¹ both at low and high temperatures. From a theoretical point of view, some papers have discussed the thermal expansivity of periclase, both with a simplified Grüneisen³² and a full quasi-harmonic approach.^{18,20,33} In particular, Karki *et al.*¹⁸ reported LDA results, up to 3000 K, where a good description was obtained up to about 700 K. Wu *et al.*³³ reported the LDA thermal expansion of MgO by discussing a semiempirical anharmonic correction³⁴ to the free energy that allowed for obtaining a good description of $V(T)$ up to 3000 K. Oganov and Dorogokupets²⁰ reported GGA results, up to 3000 K, that were systematically underestimating the experimental thermal expansion, even at very low temperatures. Both studies discussed a large effect of explicit anharmonic terms above about 500 K. For CaO, less experimental data are reported in the literature.^{23,29} To the best of our knowledge, only one theoretical study reported some LDA values of thermodynamic properties of lime, as computed at just three temperatures (300, 1000 and 2000 K).¹²

Both the numerical accuracy of the present implementation and the validity domain of the QHA are here critically discussed for the two systems. Special attention is devoted to the investigation of the effect on computed quasi-harmonic properties of: i) the size of the supercell that is used for the lattice dynamical calculation (*i.e.* the sampling of the phonon dispersion in the Brillouin zone); ii) the adopted approximation to the DFT. Five different functionals, belonging to three different rungs of “Jacob’s ladder” are explicitly considered: a LDA functional; three GGA functionals (namely, PBE, BLYP and PW91) and a global hybrid functional (namely, B3LYP). Given that the same computational methodology and setup is used for all of them, merits and limitations of different classes of functionals can be consistently discussed as regards their description of quasi-harmonic properties.

The structure of the paper is as follows: in Section II the main expressions of harmonic and quasi-harmonic properties of solids are recalled; a brief description of the structure of the revised algorithm used is given in Section III; computational details are provided in Section

IV; results on computed harmonic and quasi-harmonic properties of MgO and CaO are presented in Section V; conclusions are drawn in Section VI.

II. HARMONIC AND QUASI-HARMONIC FORMALISM

The calculation of the harmonic thermodynamic properties of crystals requires the knowledge of phonon modes over the complete first Brillouin zone (FBZ) of the system; phonons at points different from Γ can be obtained by building a supercell (SC) of the original unit cell, following a direct-space approach.³⁵⁻³⁷ The lattice vectors $\mathbf{g} = \sum_t l_t^g \mathbf{a}_t$ identify the general crystal cell where $\{\mathbf{a}_t\}$ are the direct lattice basis vectors, with $t = 1, \dots, D$ (where D is the dimensionality of the system: 1, 2, 3 for 1D, 2D, 3D periodic systems): within periodic boundary conditions the integers l_t^g run from 0 to $L_t - 1$. The parameters $\{L_t\}$ define size and shape of the SC in direct space. Let us label with \mathbf{G} the general super-lattice (*i.e.* whose reference cell is the SC) vector and let us introduce the $L = \prod_t L_t$ Hessian matrices $\{\mathbf{H}^{\mathbf{g}}\}$ whose elements are $H_{ai,bj}^{\mathbf{g}} = \partial^2 E / (\partial u_{ai}^0 \partial u_{bj}^{\mathbf{g}})$ where atom a is displaced along the i -th Cartesian direction within the reference cell and atom b is displaced in cell \mathbf{g} , along with all its periodic images in the crystal (that is in cells $\mathbf{g} + \mathbf{G}$). The set of L Hessian matrices $\{\mathbf{H}^{\mathbf{g}}\}$ can be Fourier transformed into a set of *dynamical matrices* $\{\mathbf{W}^{\mathbf{k}}\}$ each one associated with a wavevector $\mathbf{k} = \sum_t (\kappa_t / L_t) \mathbf{b}_t$ where $\{\mathbf{b}_t\}$ are the reciprocal lattice vectors and the integers κ_t run from 0 to $L_t - 1$:

$$\mathbf{W}^{\mathbf{k}} = \sum_{\mathbf{g}=0}^{L-1} \mathbf{M}^{-\frac{1}{2}} \mathbf{H}^{\mathbf{g}} \mathbf{M}^{-\frac{1}{2}} \exp(i\mathbf{k} \cdot \mathbf{g}), \quad (1)$$

where \mathbf{M} is the diagonal matrix with the masses of the nuclei associated with the $3M$ atomic coordinates where M is the number of atoms per cell. The solution is then obtained through the diagonalization of the L matrices $\{\mathbf{W}^{\mathbf{k}}\}$:

$$(\mathbf{U}^{\mathbf{k}})^\dagger \mathbf{W}^{\mathbf{k}} \mathbf{U}^{\mathbf{k}} = \mathbf{\Lambda}^{\mathbf{k}} \quad \text{with} \quad (\mathbf{U}^{\mathbf{k}})^\dagger \mathbf{U}^{\mathbf{k}} = \mathbf{I}. \quad (2)$$

The elements of the diagonal $\mathbf{\Lambda}^{\mathbf{k}}$ matrix provide the *vibrational frequencies*, $\nu_{\mathbf{k}p} = \sqrt{\lambda_{\mathbf{k}p}}$ (atomic units are adopted), while the columns of the $\mathbf{U}^{\mathbf{k}}$ matrix contain the corresponding *normal coordinates*. To each \mathbf{k} -point in the first Brillouin zone, $3M$ harmonic oscillators (*i.e.* phonons) are associated which are labeled by a phonon band index p ($p = 1, \dots, 3M$) and whose energy levels are given by the usual harmonic expression:

$$\varepsilon_m^{p,\mathbf{k}} = \left(m + \frac{1}{2}\right) \omega_{\mathbf{k}p}, \quad (3)$$

where m is an integer and $\omega_{\mathbf{k}p} = 2\pi\nu_{\mathbf{k}p}$.

Let us stress that, given the usual reciprocity between direct and reciprocal spaces, within the direct space approach that is used here, the size of the adopted SC corresponds to the sampling of the FBZ. Use of the primitive

cell would allow for the description of Γ modes only while a $3 \times 3 \times 3$ SC would correspond to a $3 \times 3 \times 3$ mesh of \mathbf{k} -points in the FBZ, for instance. Increasing the size of the SC simply corresponds to increasing the sampling of the phonon dispersion in the FBZ in reciprocal space. SCs of different size or shape do generally sample the FBZ in different \mathbf{k} -points; some \mathbf{k} -points, of course, can be sampled by different SCs (the Γ point, for instance, is sampled by all SCs). In these cases, the high numerical accuracy of the entire procedure ensures the phonon frequencies which refer to the same \mathbf{k} -points to exhibit the same values when computed with different SCs, within 0.1 cm^{-1} .

The overall vibrational canonical partition function of a crystal, $Q_{\text{vib}}(T)$, at a given temperature T , can be expressed as follows:

$$Q_{\text{vib}}(T) = \sum_{\mathbf{k}=0}^{L-1} \sum_{p=1}^{3M} \sum_{m=0}^{\infty} \exp \left[-\frac{\varepsilon_m^{p,\mathbf{k}}}{k_B T} \right], \quad (4)$$

where k_B is Boltzmann's constant. According to standard statistical mechanics, thermodynamic properties of crystalline materials such as entropy, $S(T)$, and thermal contribution to the internal energy, $\mathcal{E}(T)$, can be expressed as:

$$S(T) = k_B T \left(\frac{\partial \log(Q_{\text{vib}})}{\partial T} \right) + k_B \log(Q_{\text{vib}}), \quad (5)$$

$$\mathcal{E}(T) = k_B T^2 \left(\frac{\partial \log(Q_{\text{vib}})}{\partial T} \right). \quad (6)$$

From the above expression for $\mathcal{E}(T)$, the constant-volume specific heat, $C_V(T)$, can also be computed according to $C_V(T) = \partial \mathcal{E}(T) / \partial T$. By casting equation (4) into equations (5) and (6) one gets the following harmonic expressions:

$$S(T) = k_B \sum_{\mathbf{k}p} \left[\frac{\hbar \omega_{\mathbf{k}p}}{T \left(e^{\frac{\hbar \omega_{\mathbf{k}p}}{k_B T}} - 1 \right)} - \log \left(1 - e^{-\frac{\hbar \omega_{\mathbf{k}p}}{k_B T}} \right) \right] \quad (7)$$

$$\mathcal{E}(T) = \sum_{\mathbf{k}p} \hbar \omega_{\mathbf{k}p} \left[\frac{1}{2} + \frac{1}{e^{\frac{\hbar \omega_{\mathbf{k}p}}{k_B T}} - 1} \right] \quad (8)$$

$$C_V(T) = \sum_{\mathbf{k}p} \frac{(\hbar \omega_{\mathbf{k}p})^2}{k_B T^2} \frac{e^{\frac{\hbar \omega_{\mathbf{k}p}}{k_B T}}}{\left(e^{\frac{\hbar \omega_{\mathbf{k}p}}{k_B T}} - 1 \right)^2} \quad (9)$$

An explicit harmonic expression of Helmholtz's free energy, $F(T)$, can also be derived (see below). The HA has successfully been applied to the study of spectroscopic and some thermodynamic properties of many crystals due to its simplicity and predictive power.³⁸⁻⁴⁰ However, the limitations of the HA are well-known: zero thermal expansion, temperature independence of elastic constants and bulk modulus, equality of constant-pressure

and constant-volume specific heats, infinite thermal conductivity and phonon lifetimes, etc.^{8,9} The simplest way for correcting most of the above mentioned deficiencies of the HA is represented by the QHA, according to which, the Helmholtz free energy of a crystal is written retaining the same harmonic expression⁴¹ but introducing an explicit dependence of vibration phonon frequencies on volume:^{10,11}

$$F^{\text{QHA}}(T, V) = U_0(V) + F_{\text{vib}}^{\text{QHA}}(T, V), \quad (10)$$

where $U_0(V)$ is the zero-temperature internal energy of the crystal without any vibrational contribution (a quantity commonly accessible to standard *ab initio* simulations via volume-constrained geometry optimizations) and the vibrational part reads:

$$F_{\text{vib}}^{\text{QHA}}(T, V) = E_0^{\text{ZP}}(V) + k_B T \sum_{\mathbf{k}p} \left[\ln \left(1 - e^{-\frac{\hbar \omega_{\mathbf{k}p}(V)}{k_B T}} \right) \right], \quad (11)$$

where $E_0^{\text{ZP}}(V) = \sum_{\mathbf{k}p} \hbar \omega_{\mathbf{k}p}(V) / 2$ is the zero-point energy of the system. The equilibrium volume at a given temperature T , $V(T)$, is obtained by minimizing $F^{\text{QHA}}(V; T)$ with respect to volume V , keeping T as a fixed parameter. A volumetric thermal expansion coefficient $\alpha_V(T)$ can be defined as:

$$\alpha_V(T) = \frac{1}{V(T)} \left(\frac{\partial V(T)}{\partial T} \right)_{P=0}. \quad (12)$$

For cubic crystals, a linear thermal expansion coefficient $\alpha_l(T)$ is commonly considered which is simply $\alpha_l(T) = \alpha_V(T) / 3$. The temperature-dependent bulk modulus of the system, $K(T)$, can be obtained as an isothermal second derivative of equation (10) with respect to the volume:

$$K(T) = V(T) \left(\frac{\partial^2 F^{\text{QHA}}(V; T)}{\partial V^2} \right)_T. \quad (13)$$

From the knowledge of $V(T)$, $\alpha(T)$ and $K(T)$, the difference between constant-pressure and constant-volume specific heats can also be computed at each temperature as:⁴²

$$C_P(T) - C_V(T) = \alpha_V^2(T) K(T) V(T) T. \quad (14)$$

III. THE REVISED ALGORITHM

A fully-automated algorithm, implemented in a development version of the CRYSTAL14 program,^{43,44} has recently been presented for the calculation of all the harmonic and quasi-harmonic properties introduced in Section II which was based on the fitting of Helmholtz's free energy, $F^{\text{QHA}}(V; T)$, as a function of volume. A more accurate and general revised version of such algorithm is presented here which relies on the direct fitting of individual phonon frequencies, $\omega_{\mathbf{k}p}(V)$, versus volume. Once

phonon frequencies are known continuously as a function of volume, all other properties can be analytically derived through the expressions reported in the previous section. In order to uniquely determine the continuity of phonon frequencies among different volumes, correctly accounting for possible crossings, scalar products of the corresponding normal modes are performed; only modes belonging to the same irreducible representation are compared. The definition of both the explored volume range and the number of considered volumes has changed in order to make it as black-box as possible.

Let us briefly sketch the structure of the new algorithm. For more details one should refer to the extended description of Ref. 2. The starting structure of the system is fully-optimized using analytical energy gradients with respect to both atomic positions and lattice parameters so as to determine the zero temperature equilibrium volume, V_0 (zero-point motion effects are neglected at this stage).⁴⁵⁻⁴⁷ A volume range is defined from a $-s\%$ compression to a $+2s\%$ expansion with respect to V_0 , where N_V equidistant volumes are considered (possible values for N_V are 4, 7 and 13, corresponding to equidistances of $s\%$, $s/2\%$ and $s/4\%$, respectively). At each volume, the structure is fully relaxed via a V -constrained geometry optimization⁴⁸ and phonon frequencies are computed.^{49,50} Once all volumes have been considered, the continuity of phonon frequencies on volume is determined before individually fitting them as a function of volume with polynomial functions of different orders, up to third order. From fitted frequencies, at any considered temperature, T , the Helmholtz free energy is evaluated through equations (10) and (11) at several volumes, minimized for determining the corresponding equilibrium volume, $V(T)$ and fitted for getting $K(T)$ from its second derivative. By fitting $V(T)$ data to a polynomial function and by taking its temperature derivative, the thermal expansion coefficient $\alpha_V(T)$ of equation (12) can then be computed numerically.

The only algorithm-specific parameters whose effect on computed properties should be discussed (even though default values are provided for all of them in the implementation in the CRYSTAL program) are: i) the size of the adopted SC; ii) the amplitude of the step, s ; iii) the number of volumes, N_V and iv) the order of the polynomial fitting function for the frequencies. The effect on computed quasi-harmonic properties of these parameters will be discussed in Section V. In particular, we will see how quasi-harmonic quantities converge much faster than harmonic ones, in terms of SC size, thus making this kind of studies definitely affordable from a computational point of view.

IV. COMPUTATIONAL SETUP

All calculations are performed with a development version of the CRYSTAL14 program which works within periodic boundary conditions and adopts localized Gaussian-

type function basis sets (BS). All-electron BSs have been used of triple-zeta valence quality, augmented with polarization functions. For MgO, the TZVP basis from Ref. 51 has been used. For CaO, the corresponding BS was found to describe too poorly the valence part of the system: starting from it, two extra-polarization functions of d -type have been added for Ca (for a total of three d functions of exponents 2.5, 0.79 and 0.25 a.u.) and one extra d -type function for O (for a total of 2 d functions of exponents 1.2 and 0.25 a.u.).

As implemented in the CRYSTAL program, infinite Coulomb and exchange sums are truncated according to five thresholds (here set to 8 8 8 8 16).⁴³ Numerical integration techniques are used for the evaluation of the DFT exchange-correlation contribution (see the XXLGRID keyword in the CRYSTAL User's Manual).⁴³ The convergence of the self-consistent-field (SCF) step of the calculation is governed by a threshold on energy of 10^{-10} hartree for geometry optimizations and phonon frequency calculations. The two tolerances governing the bipolar approximation of Coulomb and exchange integrals are here set to 22 and 18, respectively (see keyword BIPOLAR).⁴³ A sub-lattice is defined for sampling the reciprocal space with a shrinking factor of 8, for SCs containing 2 and 4 atoms, that is progressively reduced as the size of the SC increases: it becomes 6 for SCs with 8 and 16 atoms, 4 for SCs containing 24, 54 and 64 atoms and 2 for SCs with 128 and 216 atoms.

Five different functionals of the DFT are considered: a local-density approximation, LDA, the Perdew-Burke-Ernzerhof, PBE,⁵² the Perdew-Wang 1991, PW91,⁵³ and the Becke-Lee-Yang-Parr, BLYP,^{54,55} generalized-gradient functionals and the hybrid Becke-three parameters-Lee-Yang-Parr, B3LYP,⁵⁶ functional with 20% of exact Hartree-Fock exchange.

V. RESULTS AND DISCUSSION

A. Periclase MgO

Before discussing how the adopted DFT functional affects computed quasi-harmonic properties (temperature evolution of volume, bulk modulus, constant-pressure specific heat) of MgO and comparing them with available experimental data, the effect of the main parameters of the algorithm introduced in Section III has to be carefully checked. The most critical among them is the size of the SC (*i.e.* size of the mesh of \mathbf{k} -points in the FBZ) used to describe the lattice dynamics of the system (*i.e.* to compute the phonon frequencies which are then used to build all the thermodynamic functions). In a previous study, where the same computational approach was applied to characterize the thermal expansion of diamond up to 1600 K and 20 GPa, it was shown that a SC containing at least 64 atoms was necessary to converge the description of $\alpha_V(T)$.² Surprisingly enough, in the present case, we find something rather different: in or-

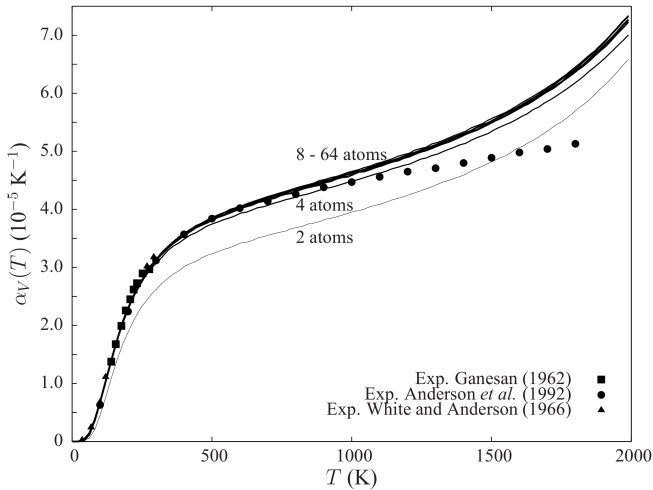


FIG. 1. Thermal expansion coefficient, $\alpha_V(T)$, of MgO, periclase, as a function of temperature. Experimental data are from Ganesan³⁰ (solid squares), Anderson *et al.*²⁴ (solid circles) and White and Anderson³¹ (solid triangles). Computed quasi-harmonic values, at PBE level of theory, are reported as continuous lines of increasing thickness as a function of the size of the adopted supercells (SC). Curves are reported for SCs containing 2, 4, 8, 16, 24, 54 and 64 atoms. $N_V = 7$ and $s = 6$.

der to converge the description of all the quasi-harmonic properties in the whole temperature range [0 K - 2000 K] for both MgO and CaO, a SC containing just 8 atoms is enough. These findings have a great computational relevance as, along with other evidences to be discussed below, they imply that a full quasi-harmonic characterization of this family of ionic systems can be performed routinely at the *ab initio* level without prohibitive costs. The effect of the SC size on the computed thermal expansion coefficient of MgO, at PBE level, is reported in Figure 1, where $\alpha_V(T)$ is reported as a function of temperature, up to 2000 K. Computed quasi-harmonic values are reported as continuous lines of increasing thickness as a function of the size of the adopted SC. Curves are reported for SCs containing 2, 4, 8, 16, 24, 54 and 64 atoms. The figure shows that the primitive cell (containing 2 atoms) is inadequate to describe $\alpha_V(T)$; a SC containing 4 atoms significantly ameliorates the description, still not being at convergence, while SCs containing 8 or more atoms provide exactly the same description. As we shall discuss below, much larger SCs are needed to converge individual harmonic thermodynamic properties such as entropy and constant-volume specific heat.

In Figure 1, three experimental datasets are also reported: by Ganesan³⁰ (solid squares), Anderson *et al.*²⁴ (solid circles) and White and Anderson³¹ (solid triangles). By comparing converged theoretical results with experimental determinations we note that: i) for temperatures up to about 1000 K, the quasi-harmonic description of the thermal expansion of MgO is in remarkable agreement with the experiment; ii) above about 1000

TABLE I. Effect of N_V and s on the computed thermal expansion coefficient, $\alpha_V(T)$, of MgO at selected temperatures (data in 10^{-5} K^{-1}). When N_V is explored, s is set to 6, whereas when s is explored, N_V is kept to 7. Calculations performed at PBE level on a SC with 16 atoms.

T	N_V			s				
	4	7	13	3	4	5	6	7
100	0.68	0.66	0.66	0.67	0.66	0.67	0.66	0.67
200	2.28	2.28	2.28	2.30	2.29	2.29	2.28	2.28
400	3.57	3.59	3.59	3.61	3.59	3.59	3.59	3.57
600	4.04	4.05	4.06	4.10	4.08	4.08	4.05	4.02
800	4.34	4.37	4.37	4.44	4.42	4.39	4.37	4.33
1000	4.64	4.65	4.66	4.80	4.75	4.69	4.65	4.61
1200	4.94	4.96	4.97	5.16	5.13	5.00	4.96	4.92
1400	5.34	5.33	5.33	-	5.60	5.41	5.33	5.29
1600	5.84	5.82	5.83	-	-	5.92	5.82	5.76
1900	6.97	6.85	6.88	-	-	-	6.85	6.78

K, while experimental data increase linearly, the QHA starts deviating from linearity and progressively diverges as temperature increases. The validity domain of the QHA for MgO appears to be limited to the [0 K - 1000 K] temperature range. Above 1000 K, neglected explicit anharmonic terms of the lattice potential play a significant role in making the thermal expansion coefficient diverge. This issue has been addressed in several studies: Karki *et al.* (2000) reported QHA results of $\alpha_V(T)$ that start diverging from molecular dynamics anharmonic ones⁵⁷ at about 700 K;¹⁸ in 2003, Oganov and Dorogokupets used QHA and a quadratic anharmonic approximation of the free energy and reported significant deviations between the two starting at about 500 K;²⁰ in 2009, Wu and Wentzcovitch reported QHA results compared with semiempirical anharmonic ones where the two determinations of $\alpha_V(T)$ deviate from each other above about 800 K.³⁴ All these studies discussed the decrease of intrinsic anharmonic terms as a function of pressure; in particular, anharmonic effects are shown to become negligible up to 3000 K for pressures above about 50-60 GPa.^{18,20,34,57}

The key part of the algorithm sketched in Section III consists in computing and fitting phonon frequencies as a function of volume. Polynomials of different order are used for the fitting. As a measure of the goodness-of-fit, we consider mode specific, R_p^2 , and average over all modes, \overline{R}^2 , coefficients of determinations (the closer to 1, the better the fitting).⁵⁸ For MgO, we find overall \overline{R}^2 coefficients of 0.992033, 0.999850 and 0.999999 for first-, second- and third-order polynomials, respectively. A cubic polynomial is then found to describe very accurately the evolution on volume of all phonon frequencies and is used for all calculations. A linear fitting, that would somehow correspond to the well-known Grüneisen

approximation, gives a poor description of the volume dependence of phonon frequencies: in particular, individual R_p^2 coefficients of the six softest frequencies ($p = 1, \dots, 6$) would be as low as 0.974165 (to be compared with 0.999995 from a cubic fitting).

As introduced in Section III, two critical algorithm-specific parameters to be investigated are: i) the range of explored volumes, defined in terms of step s and ii) the number of volumes, N_V , at which phonon frequencies are explicitly computed. A given step s defines a volume range from a minimum, V_{\min}^s ($-s\%$ of V_0), to a maximum, V_{\max}^s ($+2s\%$ of V_0), where V_0 is the equilibrium volume obtained with a standard geometry optimization. Before discussing their effect on computed quantities, let us stress that, for sake of numerical accuracy, we decided to use the present scheme just by interpolating computed phonon frequencies within the explored volume interval and not by extrapolating beyond it. It follows that the definition of s determines the maximum temperature T_{\max}^s that can be explored such that $V(T_{\max}^s) \equiv V_{\max}^s$.

In Table I, we report the computed thermal expansion coefficient, $\alpha_V(T)$ of MgO at selected temperatures, as obtained by using a different number of volumes ($N_V = 4, 7$ or 13) in a fixed range $s = 6$ and, conversely, as obtained by using always 7 volumes (*i.e.* $N_V = 7$) but exploring different ranges ($s = 3, 4, 5, 6$ and 7). It turns out that computed values are almost completely independent of N_V for all considered temperatures. This finding has, again, a great computational impact as it implies, along with previous findings on the SC size, that very simple (*i.e.* not particularly costly) calculations are required for obtaining the full quasi-harmonic description of this class of systems: just 4 phonon frequency calculations of a SC containing 8 atoms. Also the effect of s is rather small, particularly so when temperatures close to the maximum one, T_{\max}^s , are not considered and even more when temperatures below 1000 K are analyzed (*i.e.* those within the validity domain of QHA). In the Table, dashes refer to temperatures beyond T_{\max}^s for different steps s .

The effect of the adopted DFT functional on computed quasi-harmonic properties (such as the temperature evolution of volume, thermal expansion coefficient and bulk modulus) is analyzed in Figure 2 up to 1000 K. As shown before, indeed, above that temperature QHA determinations are no longer reliable. Five different functionals, belonging to three rungs of “Jacob’s ladder”, are considered: LDA, PBE, BLYP, PW91 and B3LYP. Let us stress that such a homogeneous and rigorous comparison (*i.e.* at the same computational conditions) is here addressed for the first time for ionic compounds. One of us recently reported a similar comparison for a fully-covalent system as diamond.² In the upper panel of the figure, the volume of the primitive cell is reported as a function of temperature. Experimental data, given as solid symbols, are by Anderson *et al.*²⁴ (circles), Fiquet *et al.*²⁸ (squares) and Dubrovinsky and Saxena²⁵ (triangles). The thermal expansion coefficient, $\alpha_V(T)$, is re-

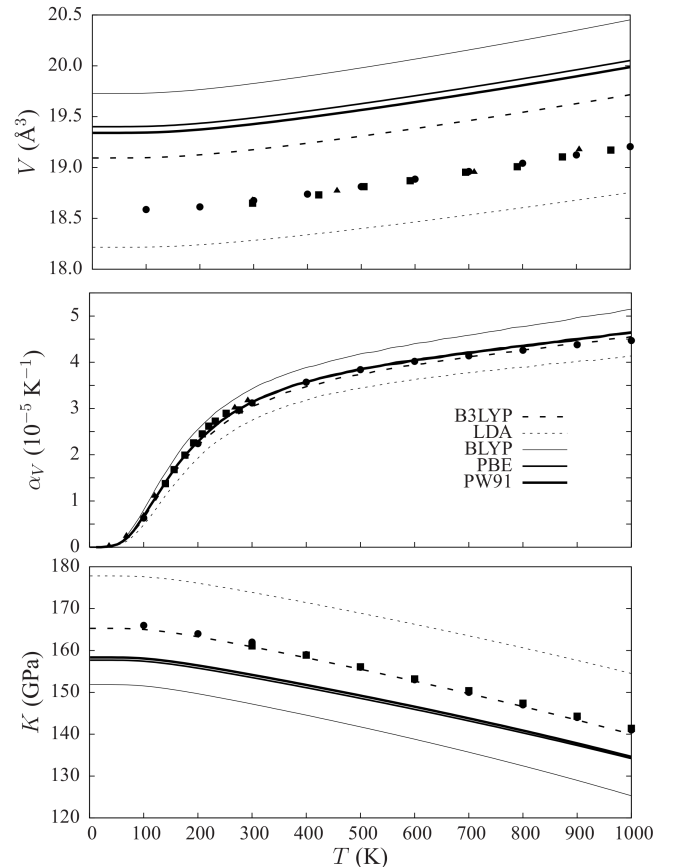


FIG. 2. Quasi-harmonic properties of MgO as a function of temperature, as computed with five different functionals of the DFT. Upper panel: volume, referring to the primitive cell (the conventional lattice parameter is given by $a = (4V)^{1/3}$); experimental data by Anderson *et al.*²⁴ (solid circles), Fiquet *et al.*²⁸ (solid squares) and Dubrovinsky and Saxena²⁵ (solid triangles). Middle panel: thermal expansion coefficient; experimental data by Ganesan³⁰ (solid squares), Anderson *et al.*²⁴ (solid circles) and White and Anderson³¹ (solid triangles). Lower panel: bulk modulus; experimental data by Anderson *et al.*²⁴ (solid circles) and Anderson and Isaak⁵⁹ (solid squares).

ported in the middle panel. Experimental determinations by Ganesan³⁰ (squares), Anderson *et al.*²⁴ (circles) and White and Anderson³¹ (triangles) are also reported. The lower panel shows the computed bulk modulus, $K(T)$ as compared with experiments by Anderson *et al.*²⁴ (circles) and Anderson and Isaak⁵⁹ (squares).

Several considerations can be made from inspection of Figure 2: i) different functionals provide rather different values of the equilibrium volume of periclase (with differences among them as large as 8%) and none of them gets closer than 2% to the experimental values; ii) LDA underestimates the volume, hybrid and GGA functionals overestimate it, more so for the latter; iii) PBE and PW91 give a very similar description to each other for all properties; iv) as regards the thermal expansion coef-

ficient, LDA is found to systematically underestimate it in the whole temperature range, PBE, PW91 and B3LYP provide results in close agreement with experimental data while BLYP overestimates it; v) different functionals provide very different descriptions of the equilibrium bulk modulus of MgO, with differences among them as large as 15%: LDA and BLYP largely overestimate and underestimate it, respectively, while B3LYP gives an excellent description of K ; vi) B3LYP also nicely describes the temperature dependence of $K(T)$, better than PBE and PW91 whose slope is too low.

Let us stress that while different functionals do provide very different values of equilibrium volume and bulk modulus, their quasi-harmonic description of the dependence on temperature of such properties is quite similar in all cases. This behavior can be traced back to their description of the phonon frequencies of the system. Different functionals do provide different values of the frequencies, with differences as large as 5%, but a very similar description of their volume dependence, which is the fundamental aspect within the QHA.

By comparing present results with those reported in a couple of previous studies where the effect of DFT functionals on computed thermal expansion of diamond² and bulk copper¹⁹ has been discussed homogeneously, some general conclusions can be drawn: i) the softer the material, the larger the deviations of $\alpha_V(T)$ among different classes of functionals (at 1000 K, the maximum deviation was reported to be about 9% for diamond, is about 25% for MgO and was reported to be about 36% for bulk copper); ii) LDA tends to systematically underestimate the volume, overestimate the bulk modulus and underestimate the thermal expansion; iii) hybrid B3LYP and GGA PBE functionals provide a reliable description of most quasi-harmonic properties. This rationalization makes questionable some of the previously reported quasi-harmonic characterizations of $\alpha_V(T)$ of MgO, as regards the effect of the adopted functional: Karki *et al.*,¹⁸ indeed, reported LDA results perfectly matching experimental values and Oganov and Dorogokupets²⁰ discussed a significant underestimation by a GGA functional.

In Figure 3, we report computed thermodynamic properties of MgO as a function of temperature, up to 2000 K: entropy, $S(T)$, constant-volume, $C_V(T)$, and constant-pressure, $C_P(T)$, specific heats. All calculations are here performed at PBE level of theory; we will explicitly discuss the effect of the adopted functional on such properties in Section VB for CaO. Both entropy and constant-volume specific heat can be derived from harmonic calculations via expressions (7) and (9). Their convergence with respect to the size of the adopted SC has to be explicitly investigated. Experimental data from Chopelas²² (solid circles) and Robie *et al.*²³ (empty circles) are reported for comparison. In the figure, we report theoretical determinations obtained with SCs of increasing size, containing 2, 4, 8, 24, 64, 128 and 216 atoms. $C_V(T)$ is shown to converge with a 64 atom SC while entropy, as generally happens, shows a slower convergence and

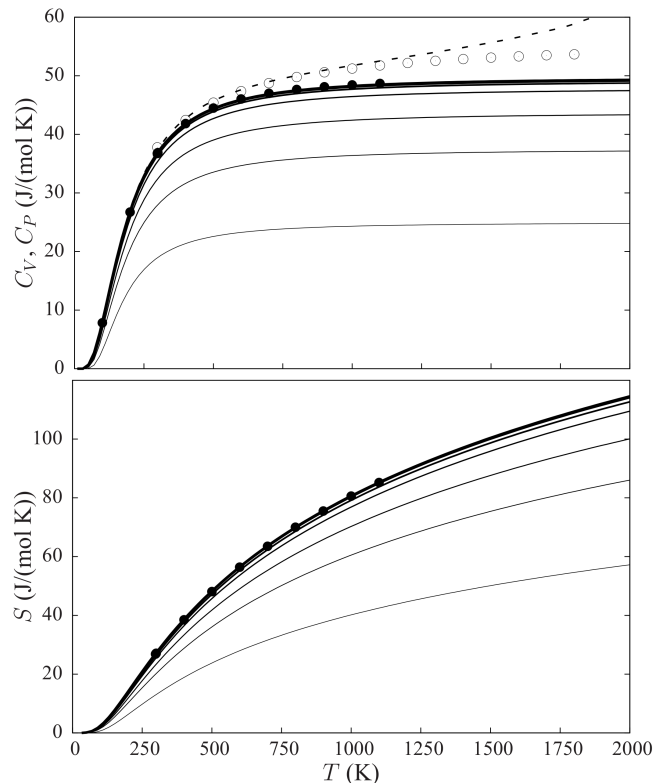


FIG. 3. Entropy (lower panel) and specific heat (upper panel) of MgO, periclase, as a function of temperature. Entropy, S , and constant-volume specific heat, C_V , are computed with harmonic expressions (7) and (9) with SCs of increasing size (continuous lines of increasing thickness) containing 2, 4, 8, 24, 64, 128 and 216 atoms. C_P (dashed line) is obtained by adding on top of the converged C_V the $C_P - C_V$ difference computed with expression (14) using quasi-harmonic quantities. Experimental data are from Chopelas²² (solid circles) and Robie *et al.*²³ (empty circles). All calculations performed at PBE level.

requires a 128 atom SC. The constant-pressure specific heat can be obtained by adding on top of the converged C_V the $C_P - C_V$ difference, computed with expression (14) using all the quasi-harmonic quantities of Figure 2. Constant-volume and constant-pressure specific heats coincide at low temperatures and start deviating from one another at about 300 K. Within the validity domain of the QHA (up to about 1000 K), the computed $C_P(T)$ is in remarkable agreement with experimental data by Robie *et al.*²³ (empty circles); above that temperature, it starts deviating, as expected from Figure 1.

B. Lime CaO

Calcium oxide has the same structure of MgO, the calcium cation being more polarizable than the magnesium one as it belongs to the fourth, instead of the third, row of the periodic table. As we will discuss below, this dif-

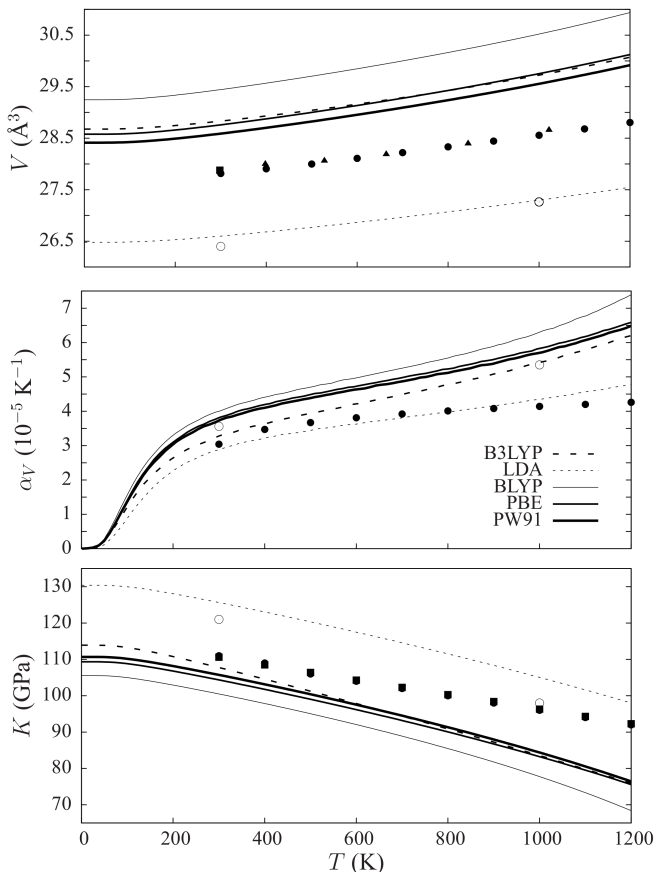


FIG. 4. Quasi-harmonic properties of CaO as a function of temperature, as computed with five different functionals of the DFT. Upper panel: volume, referring to the primitive cell; experimental data by Anderson *et al.*²⁴ (solid circles) and Fiquet *et al.*²⁸ (solid squares and triangles). Middle panel: thermal expansion coefficient; experimental data by Anderson *et al.*²⁴ (solid circles). Lower panel: bulk modulus; experimental data by Anderson *et al.*²⁴ (solid circles) and Anderson and Isaak⁵⁹ (solid squares). Previous theoretical results, at LDA level, by Karki and Wentzcovitch¹² are reported as empty circles.

ference has a huge impact on the validity domain of the QHA for the two cases. The effect on computed quasi-harmonic properties of the size of the adopted SC, the number of explored volumes, N_V , and the utilized step, s , has carefully been checked also in the case of CaO. In this respect, we find a very similar behavior to what discussed for MgO: a SC containing 8 atoms and just 4 volumes are sufficient to obtain converged results in the [0 K - 2000 K] temperature range.

The temperature dependence, up to 1200 K, of the equilibrium volume, $V(T)$, thermal expansion coefficient, $\alpha_V(T)$, and bulk modulus, $K(T)$, of CaO is reported in the three panels of Figure 4, as computed with the same five functionals of the DFT already discussed for MgO and as compared with available experimental data. As regards the relative performance of the five functionals, most of the considerations done for MgO also apply to

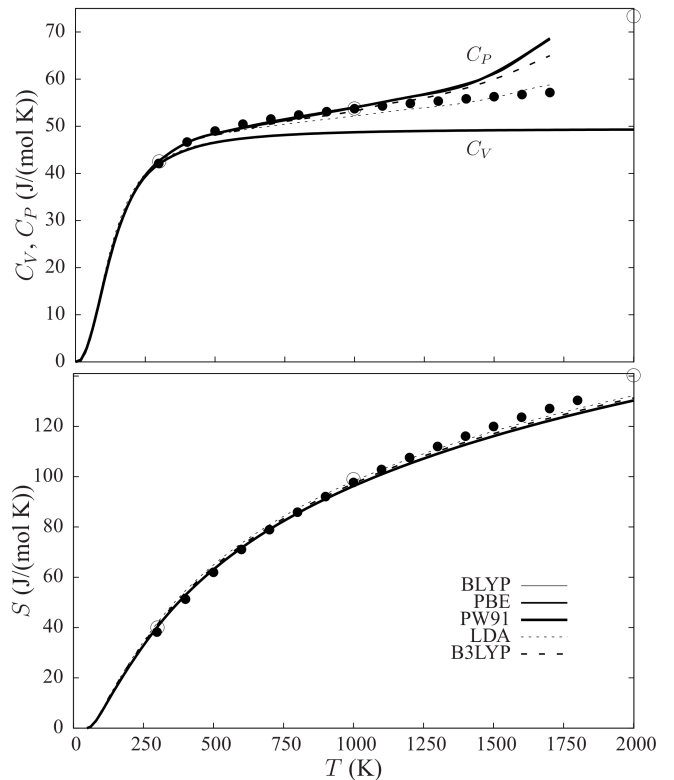


FIG. 5. Entropy (lower panel) and specific heat (upper panel) of CaO, lime, as a function of temperature, as computed with five different functionals of the DFT. Entropy, S , and constant-volume specific heat, C_V , are computed with harmonic expressions (7) and (9) with a SC containing 128 atoms. C_P is obtained by adding on top of C_V the $C_P - C_V$ difference computed with expression (14) using quasi-harmonic quantities. Experimental data are from Robie *et al.*²³ (solid circles). Previous theoretical results, at LDA level, by Karki and Wentzcovitch¹² are reported as empty circles at 300, 1000 and 2000 K.

CaO: i) LDA underestimates the volume and the thermal expansion while it overestimates the bulk modulus; ii) PBE and PW91 provide a very similar description of all quantities; iii) different functionals give very different descriptions of the equilibrium volume of CaO (with discrepancies up to 10% at zero temperature) and none of them provides a value close to the experiment.

At variance with MgO, however, as soon as the temperature dependence of these properties is considered, a severe inadequacy of the QHA can be observed in this case, even at very low temperatures. The equilibrium volume increases too rapidly with temperature for all functionals but LDA. As a consequence, the thermal expansion coefficient is systematically overestimated, even at temperatures well-below 300 K, by all those functionals (GGA and hybrids) that were giving a reliable description for MgO up to 1000 K. The dependence on temperature of the bulk modulus is also significantly wrong as it decreases with a much larger slope than expected from the experiments. These evidences are consistent with the few

data reported in the only previous theoretical investigation on thermal properties of CaO: LDA data by Karki and Wentzcovitch¹² are reported in Figure 4 as empty circles.

As a rule of thumb, we find that the validity domain of the QHA is related to the hardness of the system and, consequently, somehow related to the extent of the maximum deviation among computed $\alpha_V(T)$ with different functionals: the softer the material, the larger the deviation, the less extended the validity domain. At 1000 K, the maximum deviation (between LDA and BLYP, in this case) is about 60% for CaO. It was just 25% for MgO. In the case of CaO, the validity domain of the QHA can be approximately estimated to be restricted to the tiny [0 K - 100 K] temperature range.

Let us now discuss some thermodynamic properties of CaO: both harmonic, as entropy and constant-volume specific heat, and quasi-harmonic, as constant-pressure specific heat. A SC containing 128 atoms is enough for converging the harmonic values, as for MgO. In Figure 5, we report such properties as a function of temperature, up to 2000 K, as computed with the five different functionals of the DFT. Experimental data for entropy, $S(T)$, and constant-pressure specific heat, $C_P(T)$, are reported, from Robie *et al.*,²³ as solid circles. Previous theoretical determinations, as obtained at LDA level by Karki and Wentzcovitch¹² at three different temperatures (300, 1000 and 2000 K) are reported as empty circles. The effect of the adopted functional is seen to be extremely small on computed harmonic properties, slightly larger on the entropy than on C_V for which the five different lines in the upper panel appear almost indistinguishable. As expected from the larger differences among functionals in the description of the quasi-harmonic properties of CaO (see again Figure 4), the effect of the adopted functional is more pronounced on C_P : a quasi-harmonic property computed according to equation (14). Surprisingly enough, given the overall bad description of all quasi-harmonic properties by all functionals even at very low temperatures, $C_P(T)$ is seen to be described reasonably well by all functionals (a bit less so by LDA), up to about 1000 K. This reasonable behavior is certainly due to some compensations between over- and under-estimations of $V(T)$, $\alpha_V(T)$ and $K(T)$, which, however, we hesitate to call fortuitous due to the fact that it systematically appears with all the different functionals.

VI. CONCLUSIONS

The temperature dependence of a number of properties, both harmonic (entropy and constant-volume specific heat) and quasi-harmonic (volume, bulk modulus, constant-pressure specific heat) have been computed at the *ab initio* level of theory for two similar crystals: MgO and CaO. The harmonic description of the equilibrium lattice potential is found to give satisfactory results up to at least 2000 K in both cases. On the contrary, a very

different behavior of the quasi-harmonic approximation is observed for the two cases: it accurately describes thermal structural effects up to about 1000 K for MgO while it fails even at very low temperatures (above about 100 K) for CaO, due to the more polarizable nature of calcium cations which softens the structure and increases intrinsic anharmonic effects.

The effect of the adopted exchange-correlation functional of the DFT on computed quasi-harmonic properties has often been overlooked. In this respect, most of the previous calculations were performed at LDA level. Such an effect has here been explicitly investigated by considering five different functionals, belonging to three different rungs of the ‘‘Jacob’s ladder’’. Some general conclusions:

- Harmonic thermodynamic properties are essentially independent of the particular approximation used for the exchange-correlation functional;
- Structural quasi-harmonic properties are much more affected by the choice of the DFT functional, LDA systematically providing the lowest thermal expansion among them and generally underestimating it with respect to the experimental one;
- The softer the material, the larger the differences of the computed thermal expansion among different functionals: at 1000 K, for instance, the maximum difference on the thermal expansion coefficient is 9% for diamond² (with a bulk modulus at ambient conditions of 442 GPa), becomes 25% for MgO (bulk modulus of 162 GPa), further increases to 36% for bulk copper¹⁹ (bulk modulus of 140 GPa) and up to 60% for CaO (with a bulk modulus of 111 GPa);
- The quasi-harmonic constant-pressure specific heat is found to be less affected by the adopted functionals than its structural counterparts (volume and bulk modulus).

¹B. B. Karki, R. M. Wentzcovitch, S. de Gironcoli, and S. Baroni, *Science* **286**, 1705 (1999).

²A. Erba, *J. Chem. Phys.* **141**, 124115 (2014).

³D. Belmonte, G. Ottonello, and M. Vetuschi Zuccolini, *Am. Mineral.* **99**, 1449 (2014).

⁴D. Belmonte, G. Ottonello, and M. Vetuschi Zuccolini, *J. Chem. Phys.* **138**, 064507 (2013).

⁵G. Ottonello, M. Vetuschi Zuccolini, and D. Belmonte, *J. Chem. Phys.* **133**, 104508 (2010).

⁶J. Maul, A. Erba, I. M. G. Santos, J. R. Sambrano, and R. Dovesi, *J. Chem. Phys.* **142** (2015), in press.

⁷A. Erba, A. M. Navarrete-López, V. Lacivita, P. D’Arco, and C. M. Zicovich-Wilson, *Phys. Chem. Chem. Phys.* **17**, 2660 (2015).

⁸N. W. Ashcroft and N. D. Mermin, *Solid State Physics* (Saunders College, Philadelphia, USA, 1976).

⁹S. Baroni, P. Giannozzi, and E. Isaev, *Reviews in Mineralogy and Geochemistry* **71**, 39 (2010).

¹⁰R. E. Allen and F. W. De Wette, *Phys. Rev.* **179**, 873 (1969).

¹¹L. L. Boyer, *Phys. Rev. Lett.* **42**, 584 (1979).

- ¹²B. B. Karki and R. M. Wentzcovitch, *Phys. Rev. B* **68**, 224304 (2003).
- ¹³P. Pavone, K. Karch, O. Schütt, D. Strauch, W. Windl, P. Gianozzi, and S. Baroni, *Phys. Rev. B* **48**, 3156 (1993).
- ¹⁴J. Xie, S. P. Chen, J. S. Tse, S. de Gironcoli, and S. Baroni, *Phys. Rev. B* **60**, 9444 (1999).
- ¹⁵K. Karch, P. Pavone, W. Windl, O. Schütt, and D. Strauch, *Phys. Rev. B* **50**, 17054 (1994).
- ¹⁶Y. Ma and J. S. Tse, *Solid State Communications* **143**, 161 (2007).
- ¹⁷S. Wei, C. Li, and M. Y. Chou, *Phys. Rev. B* **50**, 14587 (1994).
- ¹⁸B. B. Karki, R. M. Wentzcovitch, S. de Gironcoli, and S. Baroni, *Phys. Rev. B* **61**, 8793 (2000).
- ¹⁹S. Narasimhan and S. de Gironcoli, *Phys. Rev. B* **65**, 064302 (2002).
- ²⁰A. R. Oganov and P. I. Dorogokupets, *Phys. Rev. B* **67**, 224110 (2003).
- ²¹M. Prencipe, M. Bruno, F. Nestola, M. De La Pierre, and P. Nimis, *Am. Mineral.* **99**, 1147 (2014).
- ²²A. Chopelas, *Phys. Chem. Miner.* **17**, 142 (1990).
- ²³R. Robie, B. S. Hemingway, and J. R. Fisher, *Thermodynamic properties of minerals and related substances at 298.15 K and 1 bar (10⁵ Pascals) pressure and at higher temperatures* (U.S. Geol. Survey Bulletin 1452, 1979).
- ²⁴O. L. Anderson, D. Isaak, and H. Oda, *Rev. Geophys.* **30**, 57 (1992).
- ²⁵L. S. Dubrovinsky and S. K. Saxena, *Phys. Chem. Miner.* **24**, 547 (1997).
- ²⁶J. Zhang, *Phys. Chem. Miner.* **27**, 145 (2000), ISSN 0342-1791.
- ²⁷R. R. Reeber, K. Goessel, and K. Wang, *Eur. J. Mineral.* **7**, 1039 (1995).
- ²⁸G. Fiquet, P. Richet, and G. Montagnac, *Phys. Chem. Miner.* **27**, 103 (1999).
- ²⁹D. K. Smith and H. R. Leider, *J. Appl. Crystallogr.* **1**, 246 (1968).
- ³⁰S. Ganesan, *Philosophical Magazine* **7**, 197 (1962).
- ³¹G. K. White and O. L. Anderson, *J. Appl. Phys.* **37**, 430 (1966).
- ³²J. Shanker, S. Kushwah, and P. Kumar, *Phys. B: Cond. Matter* **233**, 78 (1997).
- ³³Z. Wu, R. M. Wentzcovitch, K. Umemoto, B. Li, K. Hirose, and J.-C. Zheng, *J. Geophys. Res.* **113**, B06204 (2008).
- ³⁴Z. Wu and R. M. Wentzcovitch, *Phys. Rev. B* **79**, 104304 (2009).
- ³⁵A. Erba, M. Ferrabone, R. Orlando, and R. Dovesi, *J. Comput. Chem.* **34**, 346 (2013).
- ³⁶K. Parlinski, Z. Q. Li, and Y. Kawazoe, *Phys. Rev. Lett.* **78**, 4063 (1997).
- ³⁷A. Togo, F. Oba, and I. Tanaka, *Phys. Rev. B* **78**, 134106 (2008).
- ³⁸F. Pascale, C. M. Zicovich-Wilson, R. Orlando, C. Roetti, P. Ugliengo, and R. Dovesi, *J. Phys. Chem. B* **109**, 6146 (2005).
- ³⁹C. Carteret, M. De La Pierre, M. Dossot, F. Pascale, A. Erba, and R. Dovesi, *J. Chem. Phys.* **138**, 014201 (2013).
- ⁴⁰A. Erba, S. Casassa, R. Dovesi, L. Maschio, and C. Pisani, *J. Chem. Phys.* **130**, 074505 (2009).
- ⁴¹A. A. Maradudin, E. W. Montroull, and G. H. Weiss, *Theory of Lattice Dynamics in the Harmonic Approximation*, vol. 3 (Academic, New York, 1963).
- ⁴²D. C. Wallace, *Thermodynamics of Crystals* (Wiley, New York, USA, 1972).
- ⁴³R. Dovesi, V. R. Saunders, C. Roetti, R. Orlando, C. M. Zicovich-Wilson, F. Pascale, K. Doll, N. M. Harrison, B. Civalieri, I. J. Bush, et al., *CRYSTAL14 User's Manual*, Università di Torino, Torino (2014), <http://www.crystal.unito.it>.
- ⁴⁴R. Dovesi, R. Orlando, A. Erba, C. M. Zicovich-Wilson, B. Civalieri, S. Casassa, L. Maschio, M. Ferrabone, M. De La Pierre, Ph. D'Arco, et al., *Int. J. Quantum Chem.* **114**, 1287 (2014).
- ⁴⁵K. Doll, *Comp. Phys. Comm.* **137**, 74 (2001).
- ⁴⁶K. Doll, N. M. Harrison, and V. R. Saunders, *Int. J. Quantum Chem.* **82**, 1 (2001).
- ⁴⁷B. Civalieri, P. D'Arco, R. Orlando, V. R. Saunders, and R. Dovesi, *Chem. Phys. Lett.* **348**, 131 (2001).
- ⁴⁸A. Erba, A. Mahmoud, D. Belmonte, and R. Dovesi, *J. Chem. Phys.* **140**, 124703 (2014).
- ⁴⁹F. Pascale, C. M. Zicovich-Wilson, F. L. Gejo, B. Civalieri, R. Orlando, and R. Dovesi, *J. Comp. Chem.* **25**, 888 (2004).
- ⁵⁰C. M. Zicovich-Wilson, F. Pascale, C. Roetti, V. R. Saunders, R. Orlando, and R. Dovesi, *J. Comp. Chem.* **25**, 1873 (2004).
- ⁵¹M. F. Peintinger, D. V. Oliveira, and T. Bredow, *J. Comput. Chem.* **34**, 451 (2013).
- ⁵²J. P. Perdew, K. Burke, and M. Ernzerhof, *Phys. Rev. Lett.* **77**, 3865 (1996).
- ⁵³J. P. Perdew, J. A. Chevary, S. H. Vosko, K. A. Jackson, M. R. Pederson, D. J. Singh, and C. Fiolhais, *Phys. Rev. B* **46**, 6671 (1992).
- ⁵⁴A. D. Becke, *J. Chem. Phys.* **88**, 2547 (1988).
- ⁵⁵C. Lee, W. Yang, and R. G. Parr, *Phys. Rev. B* **37**, 785 (1988).
- ⁵⁶A. D. Becke, *J. Chem. Phys.* **98**, 5648 (1993).
- ⁵⁷I. Inbar and R. E. Cohen, *Geophys. Res. Lett.* **22**, 1533 (1995).
- ⁵⁸Given a set of values y_i , whose average is \bar{y} , and the corresponding set of fitted values f_i , a coefficient of determination, R^2 , measuring the goodness-of-fit can be defined as $R^2 = 1 - \frac{\sum_i (y_i - f_i)^2}{[\sum_i (y_i - \bar{y})^2]}$.
- ⁵⁹O. L. Anderson and D. G. Isaak, *Mineral Physics and Crystallography, A Handbook of Physical Constants*, vol. 3 (The American Geophysical Union, 1995).